OKLAHOMA STATE UNIVERSITY

NASA Grant NsG-454

June, 1966

PROGRESS REPORT ON NASA NsG-454 FOR

DECEMBER 1, 1965 TO MAY 31, 1966

By J. A. Wiebelt

Prepared Under Grant Number NsG-454 by
School of Mechanical Engineering
Oklahoma State University
Stillwater, Oklahoma

for

NATIONAL AERONAUTICS AND SPACE ADMINISTRATION

INTRODUCTION

This report is to cover the progress on NASA grant NsG-454 for the six month period from December 1, 1965 to May 31, 1966. The grant purpose was to examine analytically and experimentally the feasibility of using movable fins on a surface for spacecraft temperature control. For this system the geometry proposed is shown in Figure 1.

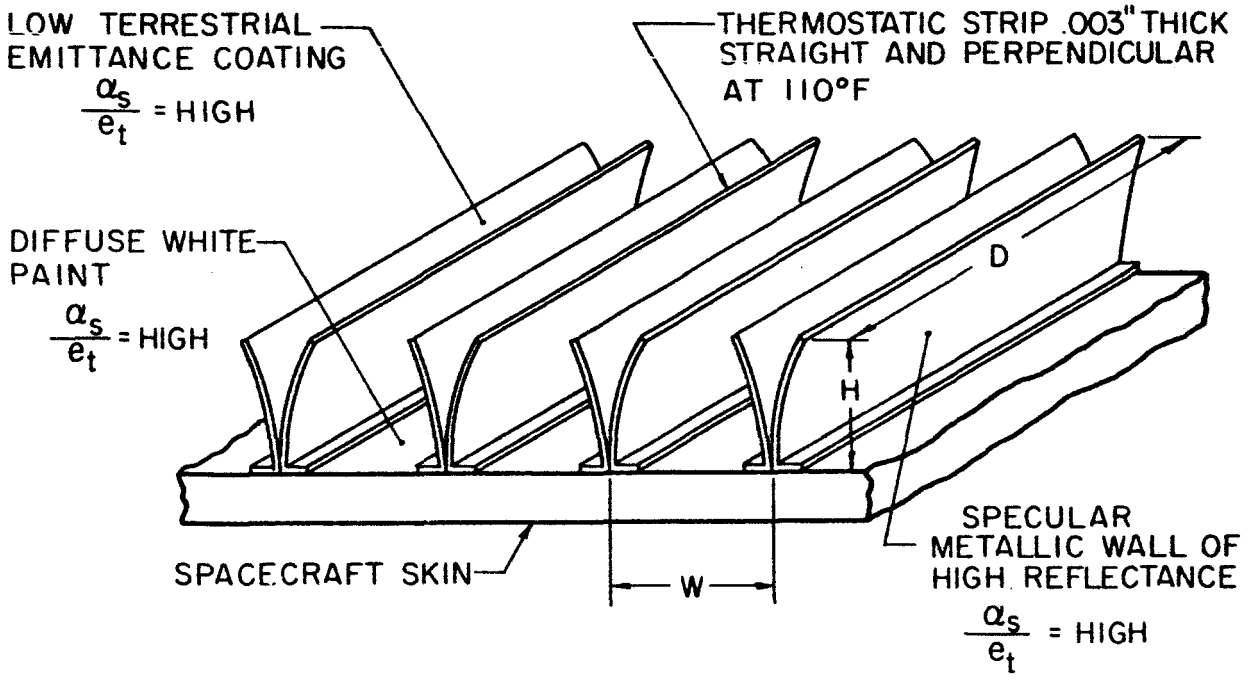

Figure 1. Temperature Control Surface

Analytical progress to date has been reported in NASA CR-91 [1]*, NASA CR-155 [2] and the semi-annual progress reports on this project. The analytical work indicated the feasibility of a certain amount of temperature control using the bi-metallic thermostatic fins. Initial experimental work indicated difficulties which were not evident from analytical considerations. Basically these difficulties consisted of thermal coupling of the fin system to the solar irradiation rather than coupling to the simulated spacecraft skin. Since the fins change position with a change of fin temperature, the control of surface properties was dependent on the solar environment rather than the spacecraft skin temperature. Since this problem relates to the conduction of energy from the spacecraft skin into the fins, further experimental investigation was considered necessary.

---

*Numbers in brackets refer to references at the end of the report.

In the previous six month period a small space simulator was constructed at Oklahoma State University in order to carry out experimental evaluation of the fin thermal control system. This simulator consisted of a high vacuum container with a liquid nitrogen cooled shroud and a small solar simulator. The cylindrical volume inside the cold wall liner in the chamber was 18 inches in diameter and 27 inches long. A six-inch diameter port in one end with a quartz window was used to introduce the solar simulation energy. This energy was obtained from either a 2.5 KW Mercury-Xenon lamp or a 2.5 KW Xenon lamp. Energy from the lamps is defocused with a quartz lens through the quartz window into the chamber. By changing the distance from the test position to the lamp, the energy intensity at the test object position could be changed. This uncollimated beam of energy had a uniformity across a 12-inch diameter circle of ± 3% and an equivalent solar constant of approximately 0.50 suns. Although it was feasible to increase the energy intensity by moving the lamp closer to the samples, uniformity decreased so the one-half sun simulation was accepted. No attempt was made to filter out any part of the energy from the lamps. This resulted in poor spectral match to the solar spectrum. Once again this was accepted since the spectral distribution from the two lamps was known and could be used with spectral information for the test system to evaluate results.

Fixed Fin Models

In the previous experimental work it was noted that bi-metallic or movable fins introduced so many parameters that evaluation of the analytical models was not possible. For this reason three models were constructed for initial experimental work which had fins in fixed position. These models are shown in Figures 2, 3, and 4. Three fin position angles were chosen as representative of the system when movable fins are used. These positions were: (1) fins vertical; (2) fins tilted 15° from the vertical; and (3) fins tilted 30° from the vertical. Figure 2 shows the vertical fin model mounted in the aluminum insulating box. A white painted aluminum "picture frame" top was mounted over the fins to eliminate energy loss from the crack between the fins and the aluminum foil wall. Figure 3 shows the model with fins tilted 15° and Figure 4 shows the model with fins tilted 30°. Position number 1 represented the fin position for maximum energy loss from the surface system. Position 3 represented the fin position for minimum energy loss and position 2 represented the fin position for an intermediate condition.

The models were made with aluminum base plates and aluminized plexiglas fins. Model number 1 had single one-inch by six-inch fins mounted on one-inch spacing across a six by six-inch base plate. The fins were press fit in a groove which was filled with high conductivity low vapor pressure grease. This grease was used to increase thermal contact conductance between the fins and the base plate. Models 2 and 3 were constructed the same size as model 1 and differed only in the angular position of the fins. For model 1 the fins were single sheets of 1/32-inch plexiglas mounted vertically. Models 2 and 3 fins were mounted in pairs to simulate the bimetal fins in closed and partially closed positions.

The plexiglas material used for the fins was vacuum plated with aluminum in order to get a highly reflective specular coating. After coating, a tab of

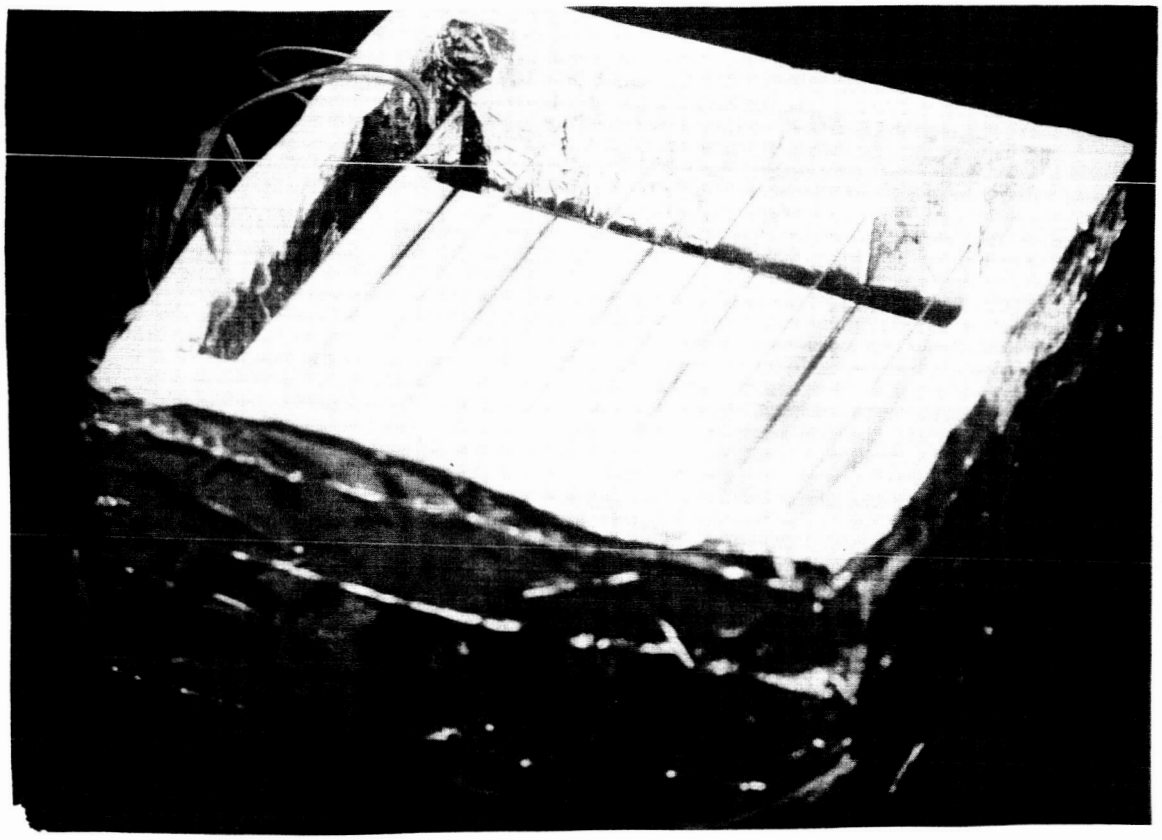

Figure 2. Fixed Fin Model - Vertical Fins

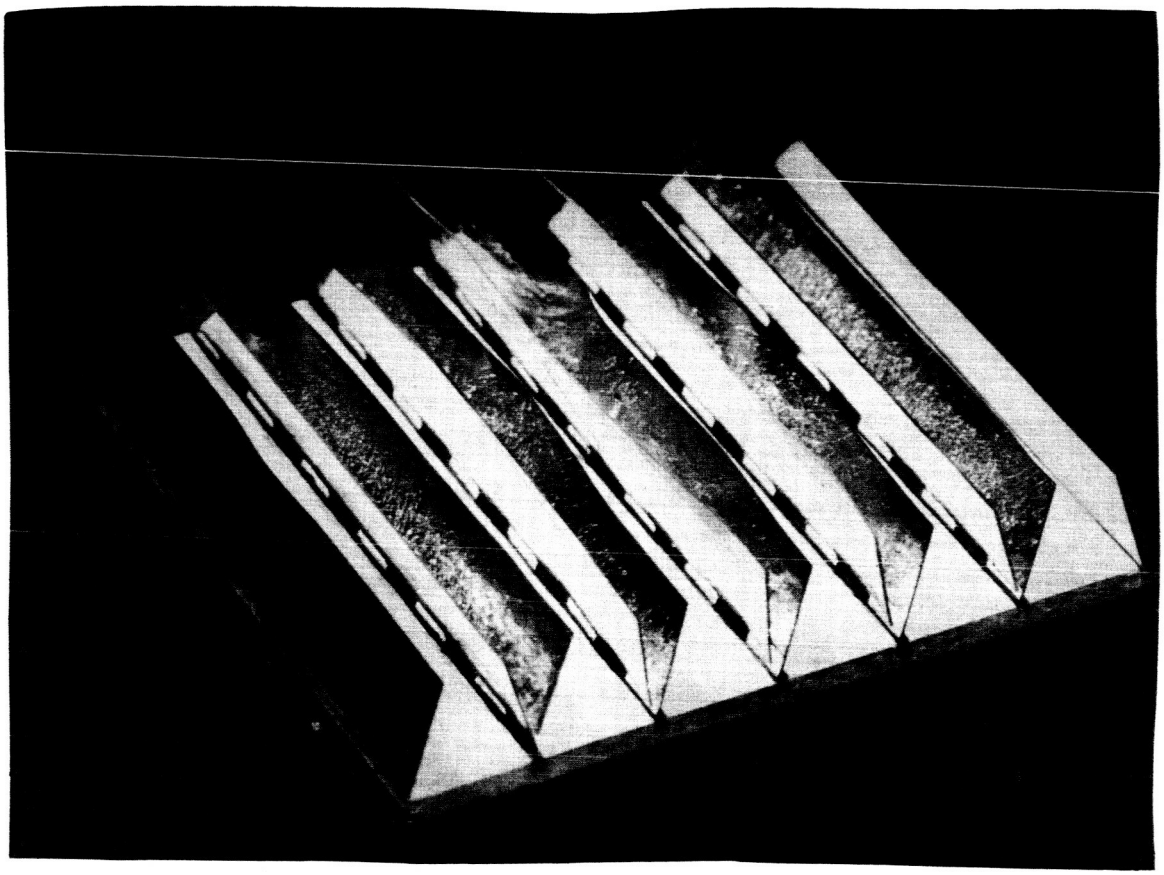

Figure 3. Fixed Fin Model - 15° Tilted Fins

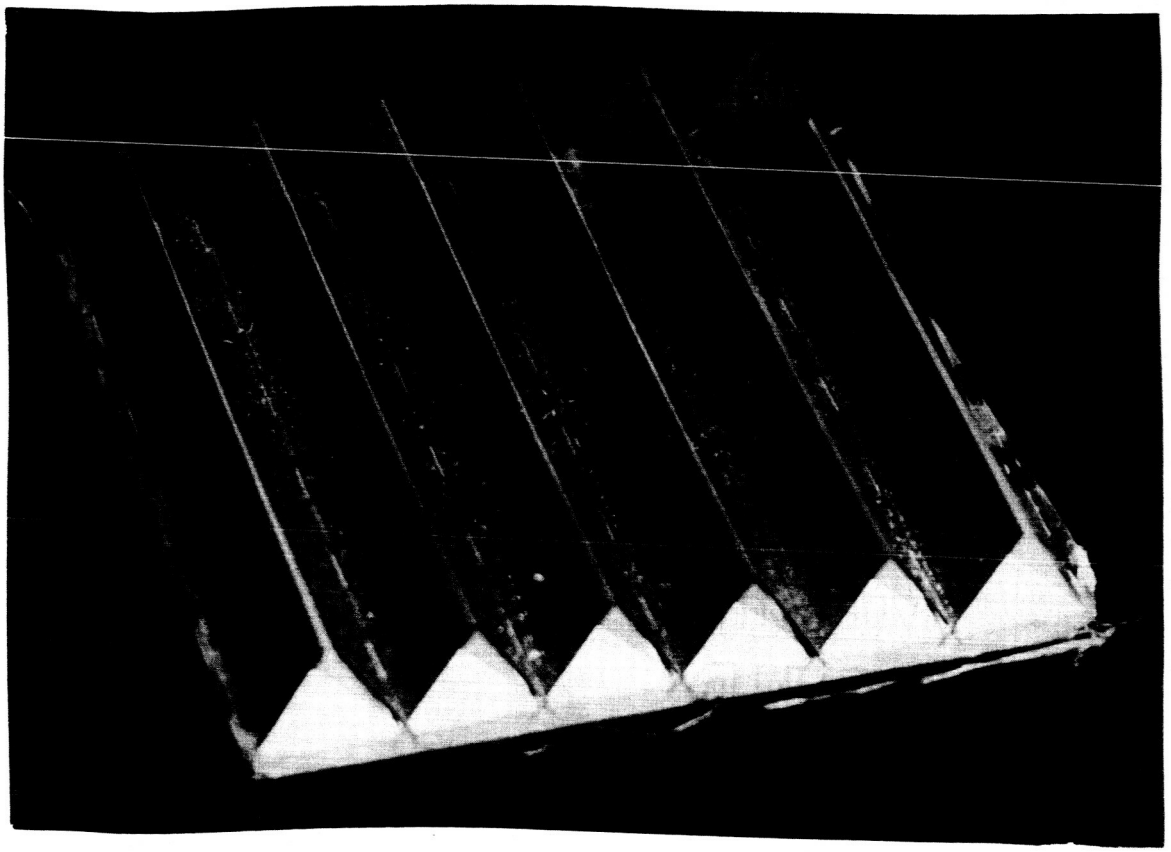

Figure 4. Fixed Fin Model - 30° Tilted Fins

typical material was used in an integrating sphere reflectometer to determine the quality of the coating. The spectral reflectance of this material is shown in Figure 5. As can be seen from the reflectance data the coated fins closely approximate well-polished aluminum.

A base plate coating with small α/ε ratio was required for the rejection of energy in the fully open position. This required a good white spacecraft paint. For this purpose the base plate was coated with about 10 mils thickness of Dow Corning Aerospace Sealent Q-90-090. The spectral reflectance of this coating material was measured using an integrating sphere system. Results of this measurement are shown in Figure 6. It was also necessary to measure the emittance since data was not available for the paint. Several measurements of this paint and a companion paint designated Q-92-007 were made. These measurements indicated a strong dependence of emittance on the coating thickness. Emittance values ranging from 0.92 to 0.76 were obtained by calorimetric methods. The larger emittance values were obtained with coating thickness of 0.019 inches and the smaller value with coating thickness of about 0.003 inches. The coating, approximately 0.010 inches thick, applied to the base plate was assumed to have an emittance of approximately 0.88.

From the spectral reflectance data, this coating had a calculated solar absorptance of 0.17. This value could not be used with the simulator since the spectral characteristics of the Xenon or mercury-xenon lamps did not match the solar spectrum. With this data the absorptance of the paint for irradiation from the mercury-xenon lamp was calculated to be 0.42 and for the xenon lamp 0.14. The extreme variation of this value indicates the importance of spectral match for solar simulation. All of these results were obtained for a very heavily coated aluminum sample. The solar absorptance of this material with thinner coatings is expected to be somewhat lower than these values.

Experimental Model Arrangement

Each of the models was prepared for testing by mounting the model in a multiple layer aluminum foil shield. This shield can be seen around model number 1 shown in Figure 2. This shield system was analyzed and examined experimentally in the previous six month progress report. By using nine layers of aluminum foil separated by porous cloth, the energy loss from the test apparatus could be evaluated from data obtained experimentally. Energy input to the fin system was accomplished by taping an electric resistance wire grid to the base plate. This heater was constructed of multiple layers of mylar adhesive tape. It was found necessary to paint the heater and base plate surfaces which faced each other with black paint to increase the heat transfer coefficient. Before painting, heater temperatures were about 200°F higher than plate temperatures. After painting, the temperature difference between the heater and base plate was reduced to approximately 30°F. Since the energy lost through the insulation ultimately depends on the heater temperature, it was desirable to maintain this as low as possible. Although it was not done, it may be observed that aluminum plating of one side of a mylar tape heater with black paint on the other side will direct energy flow out the black side in a vacuum.

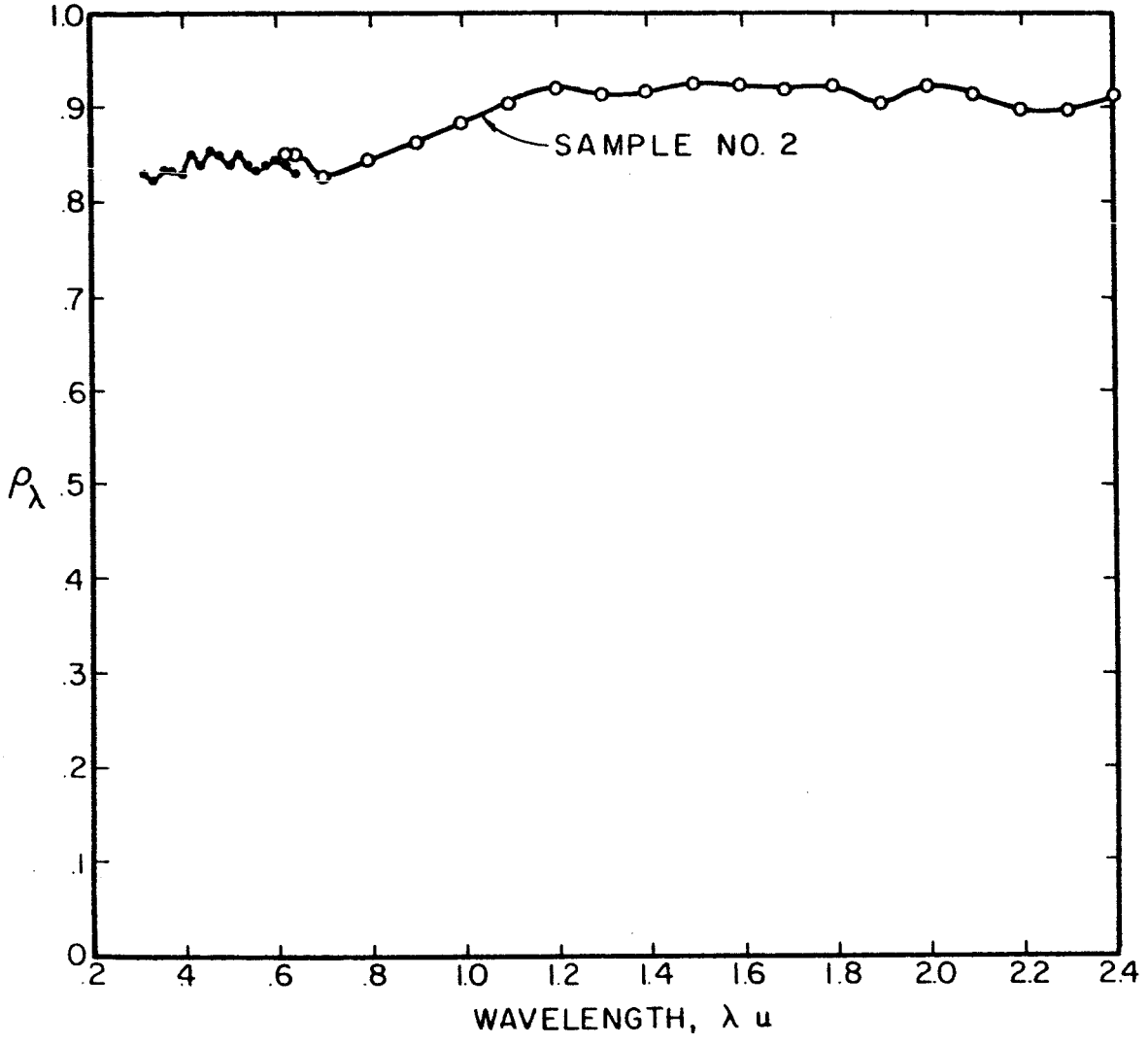

Figure 5. Monochromatic Reflectance of Aluminized Plexi-Glas

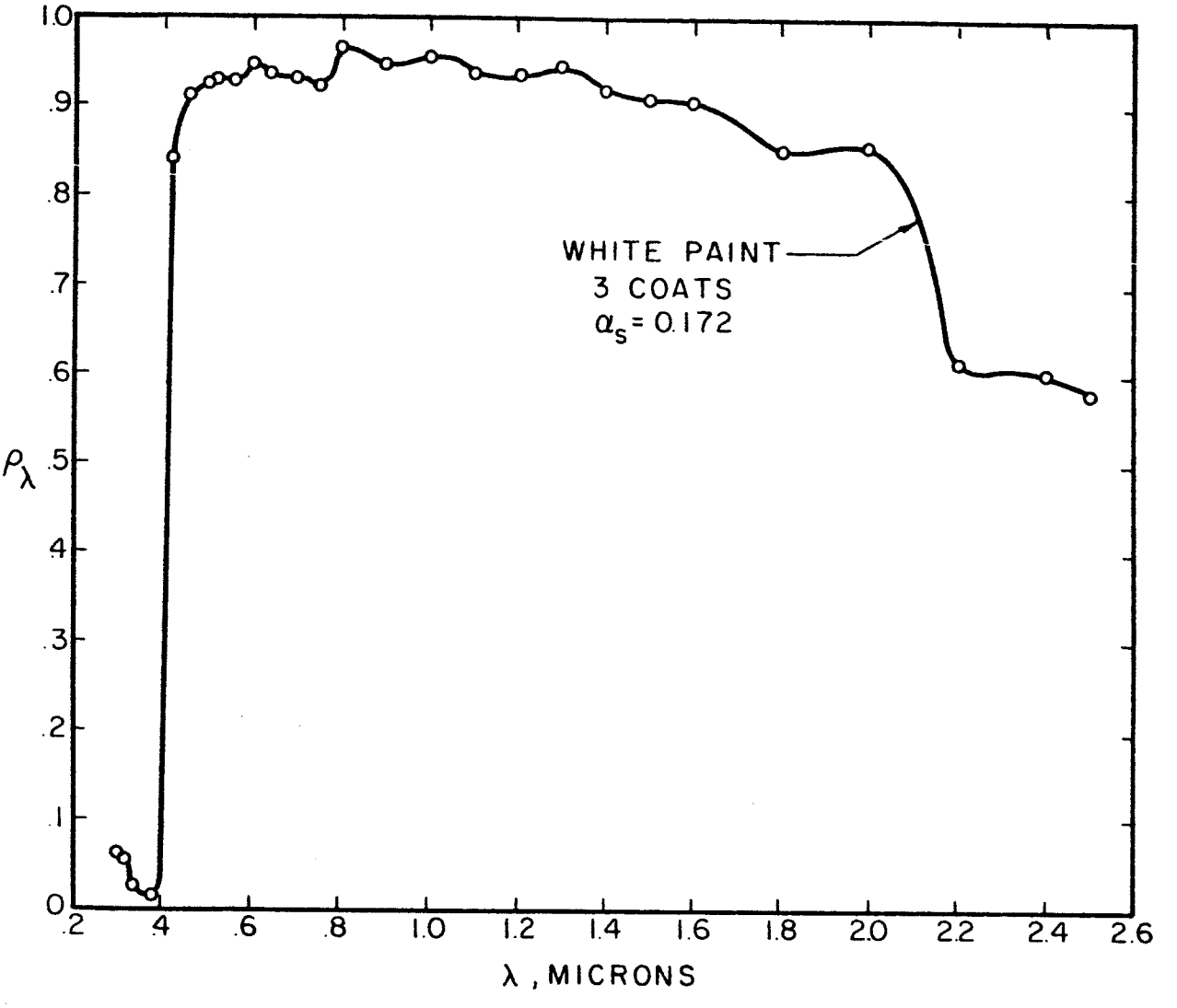

Figure 6. Monochromatic Reflectance of Dow-Corning Spacecraft Dispersion Coating - 3 Coats Brushed on Aluminum

The fin system in the insulating box was mounted in a frame and supported by four nylon cords. The nylon was used to reduce energy conducted along these supports. A typical arrangement of this type is shown in Figure 7.

Copper-constantan thermocouples were installed in two locations on the base plate, on one of the fins, and in four locations on the insulation box. The base plate temperature measurements were made along a centerline of the plate, two inches in from each edge. These thermocouples were peened into the aluminum plate on the side next to the heater. A single thermocouple was mounted on a fin half the distance from the base plate to fin top. This thermocouple was located on a centrally located fin. The thermocouples located on the insulation box were placed as described in the previous report, i.e, one located centrally on the wall, one located on the outside of the back. These thermocouples were required to evaluate the energy loss through the insulating box.

All thermocouple and heater lead wires were polished to reduce the energy loss along these wires. They were also chosen as small as practical for the same reason. For thermocouples 30 gage wire was used and for heater leads 24 gage was used. Electrical potential measurement leads were also 30 gage.

Experimental Method

After installing the model in the insulating box and the support frame, the model was mounted in the simulation chamber such that the front faced the six-inch diameter quartz window. In order to reduce the energy incident from warm surfaces, a front plate was installed on the nitrogen cooled shroud. This plate had a six-inch diameter opening facing the uncooled quartz window.

After the models were installed, the chamber was pumped down to a pressure of approximately 10^{-6} torr. Liquid nitrogen was introduced in the shroud and after a six hour cool-down period the shroud temperature was 160°R. During this period, the solar simulator was calibrated externally. This was accomplished by using a Hy-Cal pyroheliometer and two filters. The filters were used to determine the fraction of the energy in the ultraviolet region and to obtain qualitative information on the spectral distribution. After the shroud was cooled, the heater was set for a steady state, no sun thermal equilibrium run. Heater power was adjusted to obtain a base plate temperature of approximately 100°F. After thermal equilibrium was reached, the solar simulator was turned on and the heater power was reduced. The heater input power was adjusted to obtain a base plate temperature equal to the value obtained in the test without the solar irradiation. This was done in an attempt to equalize losses in the two cases. Generally, it was not possible to obtain equal temperatures, although in the case of the model with vertical fins the temperature difference was only 1°F. This experimental technique was used for the vertical fin model and for the model with fins tilted 15°. Solar irradiation was not used for the model with fins tilted 30°. This was because such a fin position would not be expected when in direct sunlight.

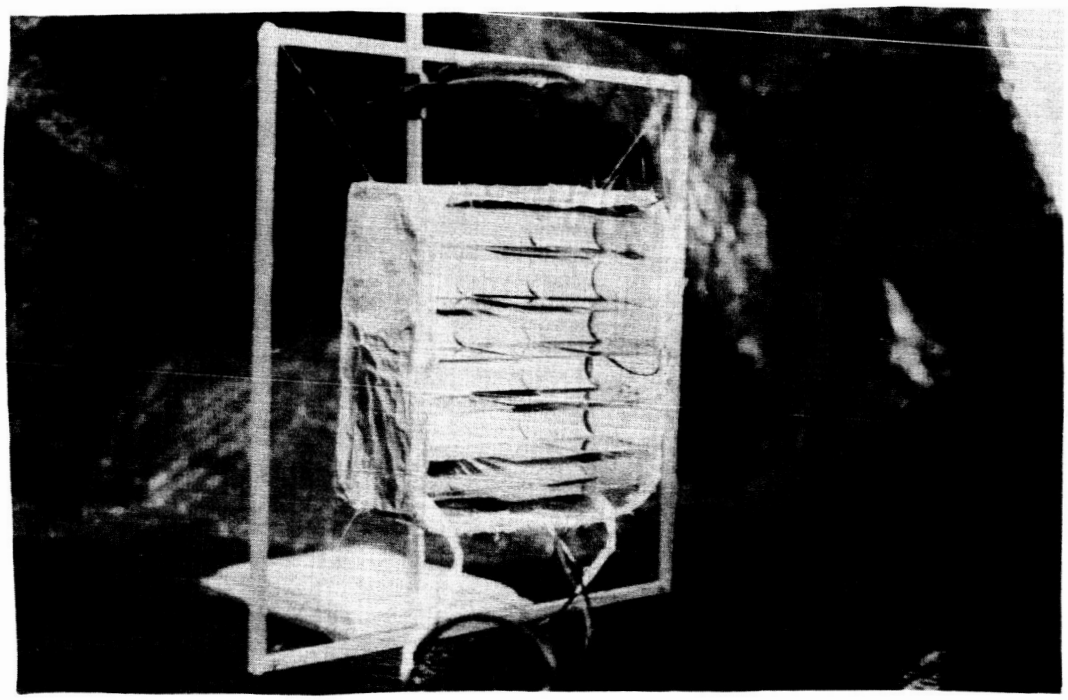

Figure 7. Fins in Test Fixture

Experimental Results

The results of nine tests are shown in Table I. Thermocouple locations are indicated in Figure 8.

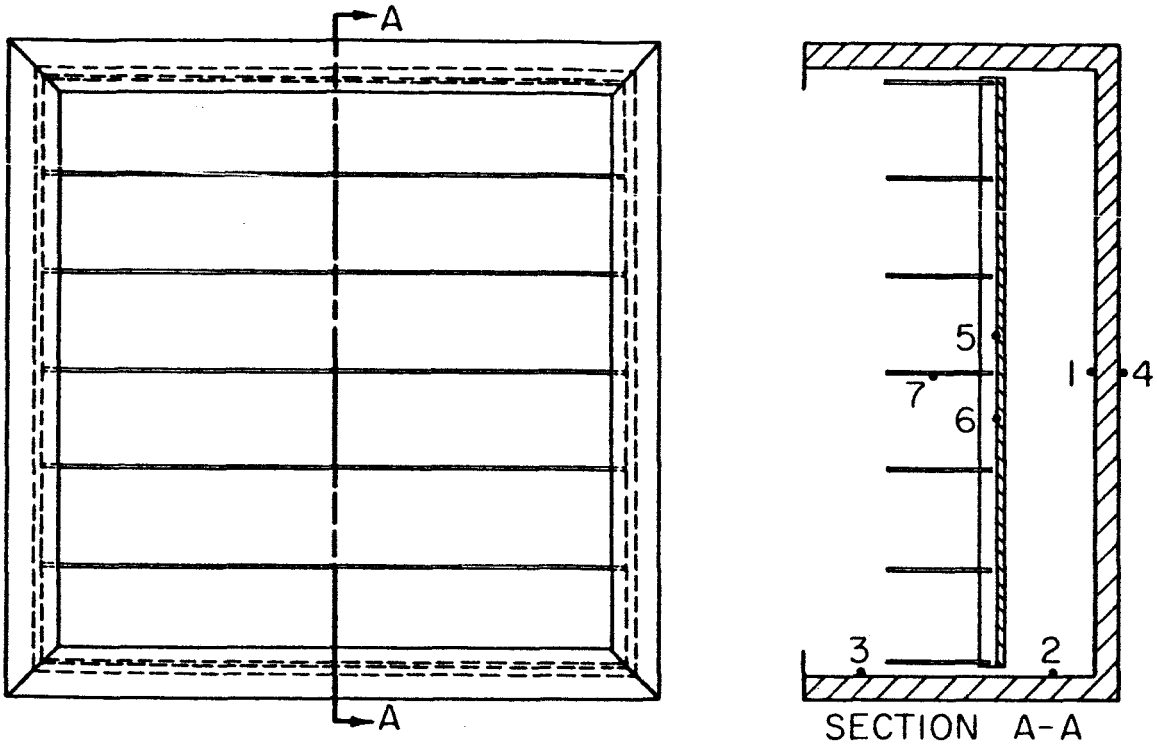

Figure 8. Thermocouple Locations

These temperatures, power inputs, and solar simulation quantities are uncorrected. The energy balance for the spacecraft skin system requires corrections for energy loss through the insulating box, along the thermocouple leads, along the heater leads, and a cavity loss.

Insulating box loss. The loss through the insulating box back and sides was determined from the temperatures measured by experimental evaluation of the insulating quality of the box. This set of experiments was discussed in the progress report for the previous six months. Basically, two identical insulating boxes were built and sandwiched around a heater element. The energy flow from the heater went through each half, assumedly symmetrically, and the temperatures were measured. From the measured temperatures and the energy input, the effective conductance of the box could be determined. In order to eliminate temperature dependence, an effective radiative constant was determined from the data.

Results of the insulating box loss for each of the tests are summarized in Table II.

Thermocouple and heater lead loss. Each of the wires leading into the insulating box conducted energy away from the system. These lead wires are very

TABLE 1

EXPERIMENTAL RESULTS

Test No.	Fin Angle Degrees	Power Input Watts	Solar Constant Eq. Suns	Temperatures °F								
				No. 1	No. 2	No. 3	No. 4	No. 5	No. 6	No. 7	No. 11	No. 12
1	0°	9 86	0	84	29	5	-194	74	74	31	-299	-300
2	0°	1.73	0.44 Hg-Xe	149	135	120	-130	99	99	148	-298	-296
3	0°	10.04	0	119	71	34	-125	98	97.6	57	-300	-303
4	0°	3.59	0.48 Xe	138	127	103	-53	98.5	98.4	128	-300	-302
5	15°	6.45	0	38	59	-17	-155	90.5	90	60	-300	-301
6	15°	0	0.48 Xe	125	135	74.5	-82.5	111.5	111.5	182	-291	-292
7	30°	3.41	0	14	33	-15	-214	103	102.5	-	-298	-298
8	30°	4.13	0	35.5	56	2	-224	128	128	-	-295	-295
9	30°	5.45	0	54	78	18	-220	146	147	-	-292	-292

TABLE 2

EXPERIMENTAL ENERGY LOSS

Test No.	Insulating Box Loss Btu/hr	Lead Loss Btu/hr	Cavity Loss Btu/hr
1	1.04	0.473	0
2	2.03	0.515	0
3	1.21	0.515	0
4	1.51	0.515	0
5	0.809	0.494	0
6	1.07	0.543	0
7	0.808	0.522	6.32
8	0.979	0.585	7.59
9	1.14	0.634	8.97

long compared to their diameter and were therefore considered as infinitely long radiating pin fins. The energy loss from such a pin fin is given by the following equation.

$$q = [2/5\ p\epsilon k A_c\ \sigma T^5]^{\frac{1}{2}}$$

where

- p is the wire perimeter or πD
- ϵ is the emittance of the wire surface
- k is the wire thermal conductivity
- A_c is the cross-sectional area of the wire or $\pi D^2/4$
- σ is the Stephan-Boltzmann constant
- T is the base temperature of the wire

The total energy loss by thermocouple lead wire and heater potential tap lead wires is tabulated in Table 2.

Cavity loss. In the case of tests 7, 8, and 9 a one-quarter inch gap around the model, that is between the model and the insulating box, existed. This gap radiated energy out the front of the insulating box. For tests 7, 8, and 9 this cavity was assumed to be radiating energy away from the system like a black body at the temperature of the box as measured at the back of the cavity. These losses are tabulated in Table 2. Upon recognition of the magnitude of these losses, the picture frame shield as shown in Figure 2 was installed for all other tests, i.e., for tests 1 through 6.

Analytical Method

The basic reason for the experimental work conducted was to determine the suitability of the analysis techniques. These techniques have been described in detail in references 1 and 2 and will be repeated only briefly here.

Basically, the system was assumed to have a configuration as shown in Figure 9.

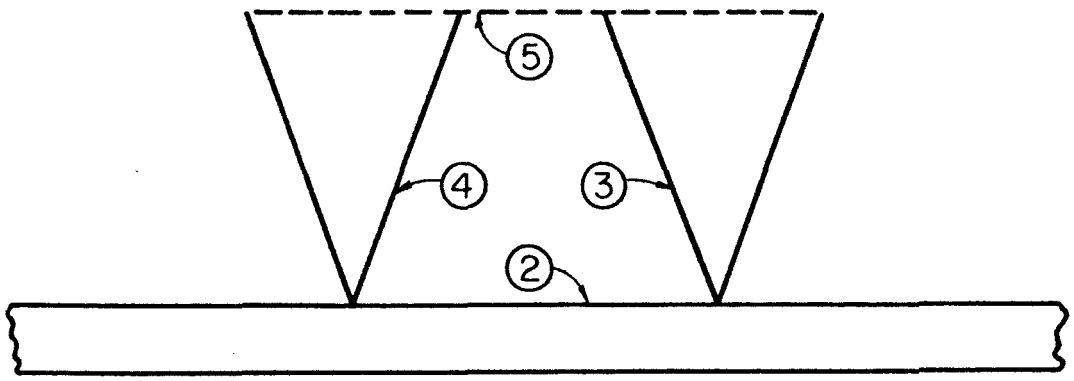

Figure 9. Surface Identification for Fin Analysis

Surface 2, the white paint coated surface, was assumed to emit and reflect in a perfectly diffuse manner. Surfaces 3 and 4, the aluminized inner surface of the plexiglas fins, were assumed to emit diffusely and reflect specularly. Then using a standard analysis technique for enclosures which include plane specular reflectors and diffuse emitters, the radiant energy exchange using gray surface assumptions was calculated. Since several surface temperatures were anticipated, radiant exchange factors as originally defined by H. C. Hottel [3] were used. These values were obtained by solving a series of linear algebraic equations formed by considering the energy incident and energy leaving each surface element.

The results of this analysis are tabulated in Table 3. Each script $\mathcal{F}$ value listed is calculated assuming no more than four "bounces" for a given ray. This was considered satisfactory for all cases, although many more reflections might be included for the case where the cavity formed is a rectangle.

The solar energy band analysis could not be accomplished using script $\mathcal{F}$ techniques. This was because the energy leaving a surface in the wavelength interval of the solar energy consisted of reflected solar energy. The exchange

TABLE 3

TABULATED RESULTS

Run No.	Calculated Energy Emitted Btu/hr	Calculated Energy Absorbed Btu/hr	Net Energy Btu/hr	Measured Net Energy Btu/hr
1	29.68	----	29.68	32.04
2	37.50	25.60	11.90	3.36
3	35.42	----	35.42	32.51
4	36.90	13.35	23.55	10.23
5	21.27	----	21.27	20.71
6		Model Destroyed in Test		
7	5.02	----	5.02	3.99
8	5.90	----	5.90	4.94
9	6.54	----	6.54	7.86

factor technique required the use of surface emission which was not present. For this reason solar energy balances were carried out using the net energy technique. This technique consists of an energy balance for each surface in the form

$$q'' = G - J$$

where

G is the irradiation

J is the radiosity

When considering solar energy, the total emissive power was considered to be zero.

Calculation details are discussed in the appendix.

Conclusions

Experimental verification, within expected accuracy, was shown for the calculation of the energy emitted by the fin models. This was evidenced by the close correspondence between the calculated net energy loss and the measured net energy loss. Runs 1 and 3 had errors of -7.4% and + 9.0%. These two runs were for a model with fins normal to the bare surface. Run 5 had an error of + 2.7%. This run was for a model in which the fins were inclined 15° from the bare surface normal. In runs 7, 8, and 9 the errors were respectively

+ 25.8%, + 19.8%, and -16.8%. Each of these runs were for a model with fins inclined 30° from the bare surface normal.

The excellent results for run 1, 3, and 5 required little discussion. Actually these runs were made at a later time than the runs numbered 7, 8, and 9. In the earlier runs it was necessary to correct for a loss due to a small gap between the base plate and the insulating box. When runs 1, 3, and 5 were made, an aluminum picture frame was installed which shielded this gap.

In the case of the runs without the shield over the gap, a loss of very significant magnitude had to be calculated. This was accomplished using a simple black cavity assumption and was strongly dependent on the cavity temperature. Since several temperatures were measured for the cavity, a question arose as to which temperature should be used. After consideration of the portion "seeing" out through the gap, it was decided to use the temperature of the inside back surface of the insulating box. Although this was the most logical choice, the actual temperature could have been considerably different than the value chosen. This variation could easily account for the one Btu per hour difference noted between calculated and measured values in these runs.

When tests were run with simulated solar energy input, the calculated values were very much in error as compared to the measured values. These errors were evidenced by the results of runs 2 and 4. The errors in these two runs were + 196% and + 129% respectively. In both of the runs, the base plate temperatures were maintained very near the base plate temperatures in runs with no solar input. This was done to make the energy loss by emission very near the energy loss by emission when solar input was not present. Calculated emitted energy values for the first four runs were very nearly the same as planned. This would indicate that the error involved in these runs was primarily involved in the solar energy analysis or experimental technique.

The analysis technique required the use of a solar absorptance value for both the base plate point and the aluminized fin surface. These values were obtained by measuring the monochromatic reflectance of the two materials and then integrating the results for absorptance. When the integration was carried out, the spectral characteristics of the Hg-Xe or Xe lamps were used as weighting functions. Both of these functions were obtained from manufacturers specifications. In the case of the white paint, large variations in absorptance were noted as a result of these spectral distributions. Since this radically affects the solar energy absorbed calculation, this value should be measured for the particular lamp in use. In future experimental work the lamp will be calibrated for spectral distribution at the model.

Another difficulty which was noted was the exact specification of the simulated solar irradiation. The simple solar simulator used in this experimental work did not have a collimated beam. The beam was simply a defocused diverging beam. When using such a system for a model with depth in the direction of the beam axis, the exact power per unit area cannot be specified. An attempt to improve this will be made by using black plate calibrations at the mean model distance.

In summary, the model runs which had no solar input corraborated analytical techniques used in radiant analysis of the complex fin system. When solar simulation was attempted, experimental values were not within acceptable limits to

corraborate the analysis techniques. The future work will be directed toward resolving the solar input problem from both the experimental and analytical directions.

APPENDIX

Calculation Techniques

The calculation of energy balances for the fin system logically divide into two parts: (1) the calculation of the energy emitted by the system, and (2) calculation of the energy absorbed by the system. These two calculations were accomplished as follows.

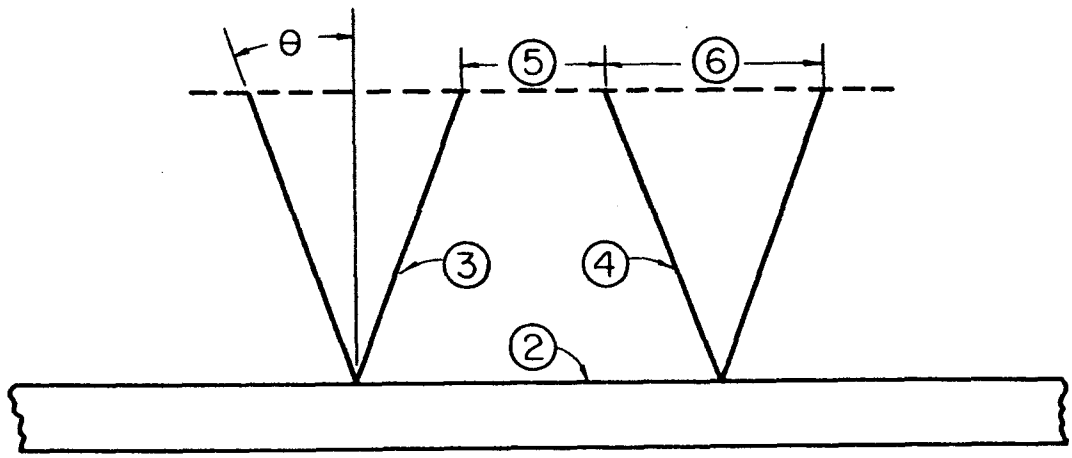

Figure 10. Surface Identification for Analysis

An energy balance across the dotted surface number 5 and 6, shown in Figure 10, must represent the energy balance for the entire system. Thus the energy passing through this surface was calculated to determine the performance of the fin system. The energy emitted was calculated by using the following equation:

$$q''net_5 = \mathcal{F}_{52} (E_{b5} - E_{b2}) + 2 \mathcal{F}_{53} (E_{b5} - E_{b3}) \quad (1)$$

$$q''net_6 = \epsilon_{eff} E_{b3} \quad (2)$$

Equation (1) represents the energy flux across the opening between fins 3 and 4. Energy flux from the groove formed by two adjacent fins is represented by equation (2). Script $\mathcal{F}$ values for use in equation (1) were obtained as

described in the previous report [4], i.e.,

$$\mathcal{F}_{25} = \frac{\epsilon_2 F_{25tot}}{1 - \rho_2 F_{22tot}} \tag{3}$$

and reciprocity $A_2 \mathcal{F}_{25} = A_5 \mathcal{F}_{52}$

$$\mathcal{F}_{35} = \epsilon_3 F_{35tot} + \frac{\epsilon_3 \rho_2 F_{25tot}}{1 - \rho_2 F_{22tot}} \tag{4}$$

and reciprocity $A_3 \mathcal{F}_{35} = A_5 \mathcal{F}_{53}$. Surface 5 was assumed to have a temperature of 0°R and the measured temperatures of surface 2 and 3 were used to calculate the total emissive powers E_{b2} and E_{b3}.

The effective emittance ϵ_{eff} used in equation (2) was obtained from the aforementioned report from Figure 10 of that report. In the case of emitted energy, a value of 0.07 was used for the emittance of the aluminized fin surfaces.

By weighting $q''net_5$ and $q''net_6$ with the proper areas, values of energy emitted were calculated, i.e.,

$$q''net\ total = A_5 q''net_5 + A_6 q''net_6 \tag{5}$$

The second part of the calculations, i.e., these for solar input, were accomplished as follows.

The solar energy gain of surface 5 was calculated using

$$q''net_5 = G_5 - J_5 \tag{6}$$

Taking the viewpoint of an observed located in the enclosure below surface 5, the radiosity, J_5, was taken as the measured irradiation from the solar simulator. The irradiation of surface 5, G_5, was calculated from the following equation.

$$G_5 = F_{25tot}\ \rho_2\ G_{solar} \tag{7}$$

where G_{solar} is the energy striking the white base surface (the solar irradiation was always normal to the base surface)

ρ_2 is the solar reflectance of the white base

F_{25tot} is given in CR-500 [4].

The energy gain by region 6 of the surface was not required in any of the calculations, since solar irradiation was used only for the case of fins normal to the surface, i.e., $\theta = 0^\circ$. However, if the fins are at an angle of $\theta > 0^\circ$, the absorptance of a specular V-groove as given in CR-500 [4] would be used for this region.

REFERENCES

1. Wiebelt, J. A., and J. F. Parmer, "Spacecraft Temperature Control by Thermostatic Fins-Analysis", NASA CR-91, August, 1964.

2. Wiebelt, J. A., J. F. Parmer, and G. J. Kneissl, "Spacecraft Temperature Control by Thermostatic Fins-Analysis Part II", NASA CR-155, January, 1965.

3. McAdams, W. H., Heat Transmission, McGraw-Hill Inc., New York (1954), Chapter 4 (by H. C. Hottel).

4. Wiebelt, J. A., C. A. Morgan, and G. J. Kneissl, "Design Considerations For Thermostatic Fin Spacecraft Temperature Control", NASA CR-500, May, 1966.